

Array Response Kernel for EEG in Four-Shell Ellipsoidal Geometry

David Gutiérrez

Centro de Investigación y de Estudios Avanzados
(CINVESTAV) Unidad Monterrey
Monterrey, N.L., 64060, México
davidgtz@cinvestav.mx

Arye Nehorai

Department of Electrical and Systems Engineering
Washington University in St. Louis
St. Louis, MO, 63130, USA
nehorai@ese.wustl.edu

Abstract— We present an analytical forward modeling solution in the form of an array response kernel for electroencephalography (EEG) assuming a four-shell ellipsoidal geometry that approximates the anatomy of the brain, cerebrospinal fluid (CSF), skull, and scalp, while a current dipole models the source. The use of an ellipsoidal geometry is useful for cases when incorporating the anisotropy of the head is important but a better model cannot be defined. The structure of our forward solution facilitates the analysis of the inverse problem by factoring the lead field into a product of the current dipole source and a kernel containing the information corresponding to the head geometry and location of the source and sensors. This factorization allows the inverse problem to be approached as an explicit function of just the location parameters, which reduces the complexity of the estimation solution search. Furthermore, we introduce an schematic representation to easily derive the conductivity function involved in our forward solution. This schematic representation generalizes the calculation of the conductivity function for any number of shells, and offers a better understanding of the effect of the geometry on the shell conductivities.

I. INTRODUCTION

Array processing methods have been developed to solve problems related to the localization of brain activity sources using electroencephalography (EEG) sensor arrays, and the solutions are useful in neurosciences and clinical applications [1]. Solution to the forward modeling problem in EEG consists of computing the electric potentials over the scalp given a current source within the brain. The forward model is necessary for solving the inverse problem (i.e., finding the current distributions using EEG measurements). Since solving the inverse problem many times involves an iterative solution of the forward problem, it is important to have an efficient form for the analytical and numerical solutions of the forward problem in order to minimize the computational burden [2].

In previous work [3], we developed analytical forward modeling solutions in the form of array response kernels for the case of EEG and magnetoencephalography (MEG) assuming a single-shell ellipsoidal geometry to approximate the anatomy of the head. In this paper, we extend those results for the case of EEG in a four-shell ellipsoidal geometry and a current dipole modeling the source of neural activity. The structure of our solution facilitates the analysis of the inverse problem by decoupling the dipole source signal (linear parameter) from the source location (nonlinear parameter). We factor the lead

field into a product of the current dipole source and kernel. This factorization allows the inverse problem to be approached as an explicit function of just the location parameters, which reduces the complexity of the estimation solution search [4].

Recently, new expressions for the electric potentials and magnetic fields in single and multi-shell ellipsoidal geometry have been developed [5]–[7]. However, these expressions are not suitable for direct use in the inverse neuroelectromagnetic problem. In Section II, we introduce the original formulation of the forward solution for EEG, while in Section III we present the algebraic steps necessary to take the forward solution into a factorized form. In Section III we also present an schematic representation for the derivation of the conductivity function involved in the forward solution. This schematic representation allows for an easy derivation of the conductivity function which can be generalized for any number of shells. In Section IV, numerical examples are used to demonstrate the applicability of our methods. Section V discusses the results and future work.

II. FORWARD MODELING SOLUTIONS

In this section, we present the derivation of the solution to the forward problem of computing the electric potential over the surface of a four-shell ellipsoidal geometry due to a current dipole source.

A. Biot-Savart-Maxwell Solution

We model the neuroelectric phenomena using the quasi-static approximation of Maxwell's equations [8]. Under this condition, the static electric field equations can be written as

$$\nabla \times \mathbf{E}(\mathbf{r}) = \mathbf{0}, \quad (1)$$

$$\nabla \cdot \mathbf{E}(\mathbf{r}) = 0, \quad (2)$$

where \mathbf{E} is the electric field and $\mathbf{r} = [r_x, r_y, r_z]^T$ is the observation point. Since \mathbf{E} is irrotational, it can be represented in terms of the electric potential v as

$$\mathbf{E}(\mathbf{r}) = -\nabla v(\mathbf{r}). \quad (3)$$

Under these conditions, the equation that relates v and the primary currents \mathbf{J}^P (considered as the sum of the *impressed*

neural current and the *microscopic* passive cellular currents) is the integral form of the Biot-Savart-Maxwell law [9]

$$v(\mathbf{r}) = \frac{1}{4\pi\sigma(\mathbf{r})} \int_V [\mathbf{J}^P(\mathbf{r}') - \sigma(\mathbf{r}')\nabla v(\mathbf{r}')] \cdot \frac{\mathbf{r} - \mathbf{r}'}{|\mathbf{r} - \mathbf{r}'|^3} dV(\mathbf{r}'), \quad (4)$$

where \mathbf{r}' is the source point, σ is the electric conductivity, and V indicates the space interior to the volume.

In the typical head model, we assume that the head may be represented by four regions, e. g., brain, cerebrospinal fluid (CSF), skull, and scalp. Another common assumption is that the conductivity $\sigma(\mathbf{r})$ is constant and isotropic within these regions. Therefore, the gradient of the conductivity is zero except at the surfaces between regions, which allows the volume integrals to be reformulated into surface integrals. Under these conditions, we can assume the regions of our head model are bounded by surfaces S_l , for $l = 1, \dots, L$, each with conductivity σ_l , going from the inner to the outer region. Furthermore, assume that the source is modeled by an equivalent current dipole (ECD), i.e.

$$\mathbf{J}^P(\mathbf{r}) = \mathbf{q}\delta(\mathbf{r} - \mathbf{r}_0), \quad (5)$$

where $\mathbf{q} = [q_x, q_y, q_z]^T$ is the dipole moment, and $\mathbf{r}_0 = [r_{0x}, r_{0y}, r_{0z}]^T$ is the source location. The ECD model is a common simplification justified when the source dimensions are relatively small compared with the distances from the source to measurement sensors [10], as it is often true for evoked response and event related experiments. Hence, substituting the ECD model in (4) and through simple vector identities, we can rewrite the volume integral as a sum of surface integrals. Therefore, the electric potential on the boundary of S_n , where $n \in l$ is given by [11]

$$v_n(\mathbf{r}) = \frac{1}{2\pi(\sigma_n^- + \sigma_n^+)} \left[\mathbf{q} \cdot \frac{\mathbf{r} - \mathbf{r}_0}{|\mathbf{r} - \mathbf{r}_0|^3} - \sum_{l=1}^4 (\sigma_l^- - \sigma_l^+) \int_{S_l} v(\mathbf{r}') \mathbf{u}'_l \cdot \frac{\mathbf{r} - \mathbf{r}'}{|\mathbf{r} - \mathbf{r}'|^3} dS_l(\mathbf{r}') \right], \quad (6)$$

where σ_l^- and σ_l^+ are the conductivities on the inner and outer sides of S_l , respectively, and \mathbf{u}'_l is the outward unit vector normal to the surface S_l at a point \mathbf{r}' .

B. Forward Solution in a Four-Shell Ellipsoidal Volume

Assume that our regions are bounded by concentric ellipsoids S_l , each defined by the following equation

$$\frac{x^2}{\alpha_{l,1}^2} + \frac{y^2}{\alpha_{l,2}^2} + \frac{z^2}{\alpha_{l,3}^2} = 1, \quad (7)$$

where $\alpha_{l,1}, \alpha_{l,2}, \alpha_{l,3}$ are the semiaxes of the l th ellipsoid. Suppose, without loss of generality, that $+\infty > \alpha_{L,1} > \alpha_{L,2} > \alpha_{L,3} > \alpha_{L-1,1} > \alpha_{L-1,2} > \alpha_{L-1,3} > \dots > \alpha_{1,1} > \alpha_{1,2} > \alpha_{1,3} > 0$. Then, equation (7) defines an ellipsoidal system [12] with coordinates (ρ, μ, ν) such that $\rho \in [\sqrt{\alpha_{*,1}^2 - \alpha_{*,3}^2}, +\infty]$, $\mu \in [\sqrt{\alpha_{*,1}^2 - \alpha_{*,2}^2}, \sqrt{\alpha_{*,1}^2 - \alpha_{*,3}^2}]$, and $\nu \in [-\sqrt{\alpha_{*,1}^2 - \alpha_{*,2}^2}, \sqrt{\alpha_{*,1}^2 - \alpha_{*,2}^2}]$, where “*” indicates that any of the ellipsoids can be considered, as all S_l are confocal.

Let us evaluate (6) using the regions defined by (7) and with $n = L = 4$. Then, the electric potential measured on the scalp is given by [7]

$$\begin{aligned} v_4(\mathbf{r}) = v(\mathbf{r}) = & \frac{3}{4\pi\alpha_{4,1}\alpha_{4,2}\alpha_{4,3}} \sum_{i=1}^3 \frac{(\mathbf{q} \cdot \mathbf{u}_i)(\mathbf{r} \cdot \mathbf{u}_i) \mathbb{I}_1^i(\rho_r)}{\mathbb{I}_1^i(\alpha_{4,1}) \mathcal{U}_1^i} \\ & - \frac{5}{8\pi\alpha_{4,1}\alpha_{4,2}\alpha_{4,3}(\gamma_1 - \gamma_2)} \sum_{i=1}^3 (\mathbf{q} \cdot \mathbf{u}_i)(\mathbf{r}_0 \cdot \mathbf{u}_i) \\ & \times \left[\frac{\mathbb{I}_2^1(\rho_r) \mathbb{E}_2^1(\rho_r, \mu_r, \nu_r)}{\gamma_1(\gamma_1 - \alpha_{4,i}^2) \mathbb{I}_2^1(\alpha_{4,1}) \mathcal{U}_2^1} - \frac{\mathbb{I}_2^2(\rho_r) \mathbb{E}_2^2(\rho_r, \mu_r, \nu_r)}{\gamma_2(\gamma_2 - \alpha_{4,i}^2) \mathbb{I}_2^2(\alpha_{4,1}) \mathcal{U}_2^2} \right] \\ & + \frac{15}{4\pi\alpha_{4,1}\alpha_{4,2}\alpha_{4,3}} \sum_{\substack{i,j=1 \\ i \neq j}}^3 (\mathbf{q} \cdot \mathbf{u}_i)(\mathbf{r} \cdot \mathbf{u}_i)(\mathbf{r} \cdot \mathbf{u}_j)(\mathbf{r}_0 \cdot \mathbf{u}_j) \\ & \times \frac{\mathbb{I}_2^{i+j}(\rho_r)}{(\alpha_{4,i}^2 + \alpha_{4,j}^2) \mathbb{I}_2^{i+j}(\alpha_{4,1}) \mathcal{U}_2^{6-i-j}} + O(\text{el}_3), \quad (8) \end{aligned}$$

where (ρ_r, μ_r, ν_r) refer to the components of \mathbf{r} in the ellipsoidal coordinate system; $\mathbb{I}_b^a(\cdot)$ is the elliptical integral of order a and degree b ; $\mathbb{E}_2^1(\cdot)$ and $\mathbb{E}_2^2(\cdot)$ are the second degree interior solid ellipsoidal harmonics of order 1 and 2, respectively; \mathbf{u}_i is the 3-dimension vector with “1” in the i th position and zero elsewhere; γ_1 and γ_2 are the roots of the quadratic equation $\sum_{i=1}^3 1/(\gamma - \alpha_{4,i}^2)$; $O(\text{el}_3)$ denotes ellipsoidal terms of degrees greater or equal to three; \mathcal{U}_b^a is the conductivity function of order a and degree b defined by (9) at the bottom of the page

$$\begin{aligned} \mathcal{U}_b^a = & \sigma_1 + (\sigma_1 - \sigma_2)({}_1\mathbb{A}_b^a) \left[\mathbb{I}_b^a(\alpha_{1,1}) - \mathbb{I}_b^a(\alpha_{4,1}) + \frac{1}{4\mathbb{A}_b^a} - \frac{1}{1\mathbb{A}_b^a} \right] + (\sigma_2 - \sigma_3)({}_2\mathbb{A}_b^a) \left[\mathbb{I}_b^a(\alpha_{2,1}) - \mathbb{I}_b^a(\alpha_{4,1}) + \frac{1}{4\mathbb{A}_b^a} - \frac{1}{2\mathbb{A}_b^a} \right] \\ & + (\sigma_3 - \sigma_4)({}_3\mathbb{A}_b^a) \left[\mathbb{I}_b^a(\alpha_{3,1}) - \mathbb{I}_b^a(\alpha_{4,1}) + \frac{1}{4\mathbb{A}_b^a} - \frac{1}{3\mathbb{A}_b^a} \right] + \frac{(\sigma_1 - \sigma_2)(\sigma_2 - \sigma_3)}{\sigma_2} ({}_1\mathbb{A}_b^a)({}_2\mathbb{A}_b^a) \left[\mathbb{I}_b^a(\alpha_{1,1}) - \mathbb{I}_b^a(\alpha_{2,1}) \right] \left[\mathbb{I}_b^a(\alpha_{2,1}) \right. \\ & \left. - \mathbb{I}_b^a(\alpha_{4,1}) + \frac{1}{4\mathbb{A}_b^a} - \frac{1}{2\mathbb{A}_b^a} \right] + \frac{(\sigma_1 - \sigma_2)(\sigma_3 - \sigma_4)}{\sigma_3} ({}_1\mathbb{A}_b^a)({}_3\mathbb{A}_b^a) \left[\mathbb{I}_b^a(\alpha_{1,1}) - \mathbb{I}_b^a(\alpha_{3,1}) \right] \left[\mathbb{I}_b^a(\alpha_{3,1}) - \mathbb{I}_b^a(\alpha_{4,1}) + \frac{1}{4\mathbb{A}_b^a} - \frac{1}{3\mathbb{A}_b^a} \right] \\ & + \frac{(\sigma_2 - \sigma_3)(\sigma_3 - \sigma_4)}{\sigma_3} ({}_2\mathbb{A}_b^a)({}_3\mathbb{A}_b^a) \left[\mathbb{I}_b^a(\alpha_{2,1}) - \mathbb{I}_b^a(\alpha_{3,1}) \right] \left[\mathbb{I}_b^a(\alpha_{3,1}) - \mathbb{I}_b^a(\alpha_{4,1}) + \frac{1}{4\mathbb{A}_b^a} - \frac{1}{3\mathbb{A}_b^a} \right] \\ & \times ({}_1\mathbb{A}_b^a)({}_2\mathbb{A}_b^a)({}_3\mathbb{A}_b^a) \left[\mathbb{I}_b^a(\alpha_{1,1}) - \mathbb{I}_b^a(\alpha_{2,1}) \right] \left[\mathbb{I}_b^a(\alpha_{2,1}) - \mathbb{I}_b^a(\alpha_{3,1}) \right] \left[\mathbb{I}_b^a(\alpha_{3,1}) - \mathbb{I}_b^a(\alpha_{4,1}) + \frac{1}{4\mathbb{A}_b^a} - \frac{1}{3\mathbb{A}_b^a} \right] \quad (9) \end{aligned}$$

and with

$${}_l\mathbb{A}_b^a = \alpha_{l,2}\alpha_{l,3}\varepsilon_b^a(\alpha_{l,1}) \left. \frac{d\varepsilon_b^a(\tau)}{d\tau} \right|_{\tau=\alpha_{l,1}}, \quad (10)$$

where $\varepsilon_b^a(\tau)$ is the interior Lamé function of order a and degree b , and τ is a nuisance variable. Details on the calculation of $\mathbb{I}_b^a(\cdot)$, $\mathbb{E}_b^a(\cdot)$, and $\varepsilon_b^a(\tau)$ are given in the Appendix B.

C. Schematic Representation of \mathcal{U}_b^a

The conductivity function (9) can be interpreted as the sum of the contributions of different paths that currents could possibly take within the various conductivity layers. Let us consider the inner layer's conductivity σ_1 as the zero level contribution. Then, the paths of first, second, and third level are shown in Figure 1 using a schematic representation. There, we can identify three possible kinds of paths:

- 1) *Downward path between consecutive layers*: The contribution of this path is characterized by the following expression

$${}_l{}_f\omega_b^a = (\sigma_{l_f} - \sigma_{l_f+1})({}_l{}_f\mathbb{A}_b^a), \quad (11)$$

where $l_f \in l$ indicates the layer where the path ends.

- 2) *Upward path between consecutive or non-consecutive layers (except the outer layer)*: The contribution of this upward path is given by

$${}_l{}_f\bar{\omega}_b^a = \frac{1}{\sigma_{l_f}} [\mathbb{I}_b^a(\alpha_{l_0,1}) - \mathbb{I}_b^a(\alpha_{l_f,1})], \quad (12)$$

where $l_0 \in l$ indicates the layer where the path starts.

- 3) *Upward path from any layer to the outer one*: This path is characterized by

$${}_{l_0}\bar{\omega}_b^a = \mathbb{I}_b^a(\alpha_{l_0,1}) - \mathbb{I}_b^a(\alpha_{4,1}) + \frac{1}{{}_4\mathbb{A}_b^a} - \frac{1}{{}_{l_0}\mathbb{A}_b^a}. \quad (13)$$

Therefore, we can easily obtain (9) using (11)-(13) and the paths in Figure 1 considering that the contributions of interconnecting paths should be multiplied, and the contributions of non-interconnecting paths should be summed. Using this method, we can easily obtain the expression of the conductivity function for any number of layers. Furthermore, this representation gives us information about the effect of the ellipsoidal geometry to the conductivities of the layers.

III. ARRAY RESPONSE KERNEL

Clearly, equation (8) is not suitable for a numerical solution of the inverse problem in EEG. Therefore, in this section we develop a novel reformulation to the forward solution based on algebraic factorizations. Our goal is then to represent the electric potential as

$$\mathbf{v}(\mathbf{r}) = \mathbf{k}^T(\mathbf{r}, \mathbf{r}_0)\mathbf{q}, \quad (14)$$

where $\mathbf{k}(\mathbf{r}, \mathbf{r}_0)$ is a 3×1 kernel vector.

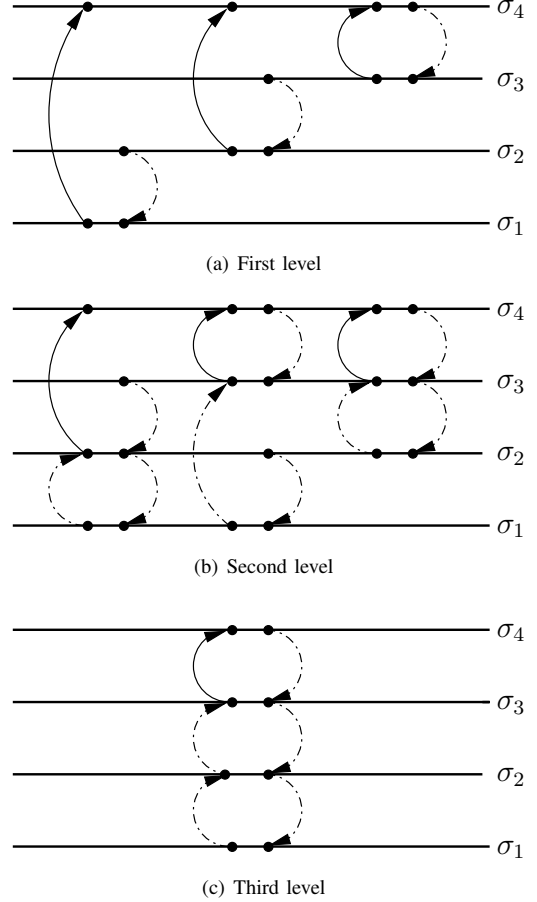


Fig. 1. Schematic representations of paths that compose the conductivity function at different contributing levels. The diagrams show the relationships between the conductivities $\sigma_1, \sigma_2, \sigma_3, \sigma_4$ (from inner to outer) in a four-shell ellipsoidal geometry. There are three kinds of interactions: downward paths (dot-dashed arrows going down), upward paths (dot-dashed arrows going up), and upward paths going to the outer layer (full-line arrows).

In order to reach the form of (14), we define the auxiliary vector $\mathbf{g}(\mathbf{r})$, and the auxiliary matrices $H_1(\mathbf{r})$, and $H_2(\mathbf{r})$ as

$$\mathbf{g}(\mathbf{r}) \triangleq \left[\sum_{i=1}^3 \frac{\mathbb{I}_1^i(\rho_r)}{\mathbb{I}_1^i(\alpha_{4,1})\mathcal{U}_1^i} \mathbf{u}_i \mathbf{u}_i^T \right] \mathbf{r}, \quad (15)$$

$$H_1(\mathbf{r}) \triangleq \frac{1}{\gamma_1 - \gamma_2} \sum_{i=1}^3 \left\{ \left[\frac{\mathbb{I}_2^1(\rho_r)\mathbb{E}_2^1(\rho_r, \mu_r, \nu_r)}{\gamma_1(\gamma_1 - \alpha_{4,i}^2)\mathbb{I}_2^1(\alpha_{4,1})\mathcal{U}_2^1} - \frac{\mathbb{I}_2^2(\rho_r)\mathbb{E}_2^2(\rho_r, \mu_r, \nu_r)}{\gamma_2(\gamma_2 - \alpha_{4,i}^2)\mathbb{I}_2^2(\alpha_{4,1})\mathcal{U}_2^2} \right] \mathbf{u}_i \mathbf{u}_i^T \right\}, \quad (16)$$

and $H_2(\mathbf{r})$ is defined by (17) shown at the bottom of the page.

$$H_2(\mathbf{r}) \triangleq \begin{bmatrix} 0 & \frac{r_x r_y \mathbb{I}_2^3(\rho_r)}{(\alpha_{4,1}^2 + \alpha_{4,2}^2)\mathbb{I}_2^3(\alpha_{4,1})\mathcal{U}_2^3} & \frac{r_x r_z \mathbb{I}_2^4(\rho_r)}{(\alpha_{4,1}^2 + \alpha_{4,3}^2)\mathbb{I}_2^4(\alpha_{4,1})\mathcal{U}_2^4} \\ \frac{r_x r_y \mathbb{I}_2^3(\rho_r)}{(\alpha_{4,1}^2 + \alpha_{4,2}^2)\mathbb{I}_2^3(\alpha_{4,1})\mathcal{U}_2^3} & 0 & \frac{r_y r_z \mathbb{I}_2^5(\rho_r)}{(\alpha_{4,2}^2 + \alpha_{4,3}^2)\mathbb{I}_2^5(\alpha_{4,1})\mathcal{U}_2^5} \\ \frac{r_x r_z \mathbb{I}_2^4(\rho_r)}{(\alpha_{4,1}^2 + \alpha_{4,3}^2)\mathbb{I}_2^4(\alpha_{4,1})\mathcal{U}_2^4} & \frac{r_y r_z \mathbb{I}_2^5(\rho_r)}{(\alpha_{4,2}^2 + \alpha_{4,3}^2)\mathbb{I}_2^5(\alpha_{4,1})\mathcal{U}_2^5} & 0 \end{bmatrix} \quad (17)$$

Therefore, using (15)–(17) in (8), and discarding the higher order terms, $\mathbf{k}(\mathbf{r}, \mathbf{r}_0)$ is expressed as

$$\mathbf{k}(\mathbf{r}, \mathbf{r}_0) = \frac{1}{c} \left[3\mathbf{g}(\mathbf{r}) - \left(\frac{5}{2}H_1(\mathbf{r}) - 15H_2(\mathbf{r}) \right) \mathbf{r}_0 \right], \quad (18)$$

where $c = 4\pi\alpha_{4,1}\alpha_{4,2}\alpha_{4,3}$.

Finally, let us consider the case when EEG measurements are obtained from an array of m sensors located at $\mathbf{r}_1, \mathbf{r}_2, \dots, \mathbf{r}_m$. Let $\mathbf{v} = [v(\mathbf{r}_1), v(\mathbf{r}_2), \dots, v(\mathbf{r}_m)]^T$ and define the $m \times 3$ array response matrix as

$$A = \begin{bmatrix} \mathbf{k}^T(\mathbf{r}_1, \mathbf{r}_0) \\ \mathbf{k}^T(\mathbf{r}_2, \mathbf{r}_0) \\ \vdots \\ \mathbf{k}^T(\mathbf{r}_m, \mathbf{r}_0) \end{bmatrix}. \quad (19)$$

Then, we can extend (14) to an array representation that contains all m kernel solutions, i.e.

$$\mathbf{v} = A\mathbf{q}. \quad (20)$$

IV. NUMERICAL EXAMPLES

We conducted a simulation for EEG measurements in the four-shell ellipsoidal model and compared the measurements to those in the classical four-shell spherical model.

In both geometries, we used an array of 61 sensors distributed in the 10-20 placement system as shown in Figure 2. In the case of the ellipsoidal model, the sensors were placed over the outer shell with semiaxes $[\alpha_{4,1}, \alpha_{4,2}, \alpha_{4,3}] = [9, 6.5, 6]$ cm, while the sensors in the spherical model were distributed on the outer sphere with radius $\varrho_4 = 9$ cm. The dimensions of the inner shells in the ellipsoidal model were chosen to be $[\alpha_{3,1}, \alpha_{3,2}, \alpha_{3,3}] = 0.9467[\alpha_{4,1}, \alpha_{4,2}, \alpha_{4,3}]$, $[\alpha_{2,1}, \alpha_{2,2}, \alpha_{2,3}] = 0.8667[\alpha_{4,1}, \alpha_{4,2}, \alpha_{4,3}]$, and

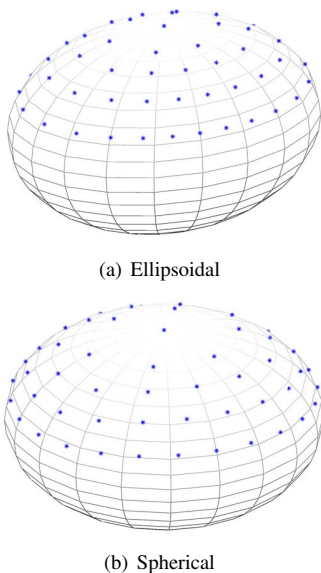


Fig. 2. Array of sensors for the ellipsoidal and spherical geometries.

$[\alpha_{1,1}, \alpha_{1,2}, \alpha_{1,3}] = 0.84[\alpha_{4,1}, \alpha_{4,2}, \alpha_{4,3}]$. Similarly, the nominal radii of the four spherical shells were chosen to be $[\varrho_1, \varrho_2, \varrho_3, \varrho_4] = [0.84\varrho_4, 0.8667\varrho_4, 0.9467\varrho_4, \varrho_4]$.

To simulate our source, we chose a current dipole located at $\mathbf{r}_0 = [0, 0, \alpha_{1,3}]^T$ in the ellipsoidal geometry, and $\mathbf{r}_0 = [0, 0, \varrho_1]^T$ in the spherical geometry (i.e. on the inner shell in any case). The dipole moment was kept constant with a value of $\mathbf{q} = [\cos \theta, \sin \theta, 0]^T$ [nA·m], with $\theta = 15$ degrees. For the conductivities, we used $[\sigma_1, \sigma_2, \sigma_3, \sigma_4] = [0.33, 1, 0.0042, 0.33]$ S/m.

Under the conditions previously described, we obtained EEG measurements for the ellipsoidal head model using the method proposed in Section III, while the forward solution in [2] was used to obtain the measurements in the four-shell spherical model. The resulting distributions of the surface potential in both geometries are shown in Figure 3.

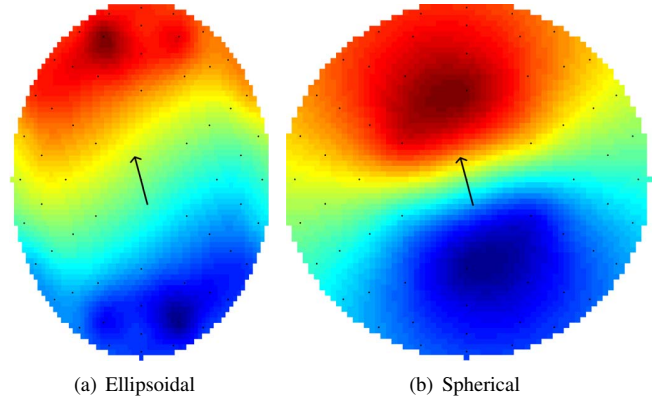


Fig. 3. Simulated surface potentials in the ellipsoidal and spherical geometries.

Our simulations show that the surface potential is more focalized in the ellipsoidal model than in the spherical one. However, the anisotropy of the ellipsoidal model “pushes” the peak in the potential further away from the source location. This effect is related to the tendency of the electric fields in an ellipsoidal volume to move towards the major semiaxis (in this case, the x axis). A similar effect has been reported in the MEG case, where the distribution of the field tends to be in the direction of the major semiaxis [13].

V. CONCLUSIONS

We presented an analytical solution to the EEG forward problem in the form of an array response kernel for the case of a four-shell ellipsoidal head model. The kernel structure of our forward solution has the potential of facilitating the solution of the inverse problem as it provides with an algebraic representation suitable for numerical implementations. We also introduced a schematic representation of the conductivity function involved in our forward solution. The schematic representation allows us to generalize the derivation of the conductivity function for any number of shells, and provides with detailed information about the effects of the geometry on the different shell conductivities.

We performed numerical simulations that seem to confirm previous findings related to the effect of the geometry of the problem on the distribution of the fields. However, further experimentation is required. Future research in this area will include more extensive applications to solve inverse problems with real data, as well as the application of our model to the estimation of conductivities in ellipsoidal geometries.

VI. ACKNOWLEDGMENT

The authors would like to thank Dr. F. Kariotou from the Hellenic Open University, Greece, for his assistance in better understanding the forward model in [6]. The work of Arye Nehorai was supported by the National Science Foundation Grants CCR-0330342 and CCF-0630734.

APPENDIX A: ELLIPSOID COORDINATE SYSTEM

The ellipsoidal coordinates (ρ, μ, ν) are connected to the Cartesian coordinates (x, y, z) through the following relationships

$$x = \frac{\rho\mu\nu}{\sqrt{(\alpha_1^2 - \alpha_2^2)(\alpha_1^2 - \alpha_3^2)}}, \quad (\text{A.1})$$

$$y = \frac{\sqrt{(\rho^2 - \alpha_1^2 + \alpha_2^2)(\mu^2 - \alpha_1^2 + \alpha_2^2)(\alpha_1^2 - \alpha_2^2 - \nu^2)}}{\sqrt{(\alpha_1^2 - \alpha_2^2)(\alpha_2^2 - \alpha_3^2)}}, \quad (\text{A.2})$$

$$z = \frac{\sqrt{(\rho^2 - \alpha_1^2 + \alpha_3^2)(\mu^2 - \alpha_1^2 + \alpha_3^2)(\alpha_1^2 - \alpha_3^2 - \nu^2)}}{\sqrt{(\alpha_1^2 - \alpha_3^2)(\alpha_2^2 - \alpha_3^2)}}, \quad (\text{A.3})$$

where the subscript of the semiaxes that indicates the shell has been dropped for notational convenience as all ellipsoids are assumed confocal.

Most of the time we want to go from cartesian to ellipsoidal coordinates. Therefore, we need to solve the nonlinear system formed by equations (A.1)-(A.3) constrained to the range in values of $\rho, \mu,$ and ν described in Section II-B.

APPENDIX B: ELLIPSOIDAL HARMONICS

In order to evaluate (8) and subsequent equations, we first need to compute the values of the elliptic integrals \mathbb{I} , and the interior solid ellipsoidal harmonics \mathbb{E} of different orders and degrees.

The elliptic integral of order a and degree b is given by

$$\mathbb{I}_b^a(\rho) = \int_{\rho^2 - \alpha_1^2}^{+\infty} \frac{d\tau}{[\varepsilon_b^a(\sqrt{\tau + \alpha_1^2})]^2 \sqrt{\tau + \alpha_1^2} \sqrt{\tau + \alpha_2^2} \sqrt{\tau + \alpha_3^2}}, \quad (\text{B.1})$$

where $\varepsilon_b^a(\cdot)$ is the interior Lamé function of order a and degree b , and τ is a nuisance variable. In our computations, we only need to evaluate ε_b^a for degrees less or equal than 2. Therefore, the interior Lamé functions [12] are given by

$$\varepsilon_0^1(\tau) = 1, \quad (\text{B.2})$$

$$\varepsilon_1^a(\tau) = \sqrt{|\tau^2 - \alpha_1^2 + \alpha_a^2|}, \quad a = 1, 2, 3, \quad (\text{B.3})$$

$$\varepsilon_2^1(\tau) = \tau^2 - \alpha_1^2 + \gamma_1, \quad (\text{B.4})$$

$$\varepsilon_2^2(\tau) = \tau^2 - \alpha_1^2 + \gamma_2, \quad \text{and} \quad (\text{B.5})$$

$$\varepsilon_2^{6-a}(\tau) = \frac{\varepsilon_1^1(\tau)\varepsilon_1^2(\tau)\varepsilon_1^3(\tau)}{\varepsilon_1^a(\tau)}, \quad a = 1, 2, 3. \quad (\text{B.6})$$

Finally, the interior solid ellipsoidal harmonics are defined as

$$\mathbb{E}_b^a(\rho, \mu, \nu) = \varepsilon_b^a(\rho)\varepsilon_b^a(\mu)\varepsilon_b^a(\nu). \quad (\text{B.7})$$

REFERENCES

- [1] C. Binnie and P. Prior, "Electroencephalography," *Journal of Neurology, Neurosurgery, and Psychiatry*, vol. 57, no. 11, pp. 1308–1319, 1994.
- [2] J. Mosher, R. Leahy, and P. Lewis, "EEG and MEG: forward solutions for inverse methods," *IEEE Transactions on Biomedical Engineering*, vol. 46, no. 3, pp. 245–259, 1999.
- [3] D. Gutiérrez and A. Nehorai, "Array response kernels for EEG/MEG in single-shell ellipsoidal geometry," in *Proceedings of the 2005 1st IEEE International Workshop on Computational Advances in Multi-Sensor Adaptive Processing*, Puerto Vallarta, Mexico, 2005, pp. 225–228.
- [4] J. Mosher, P. Lewis, and R. Leahy, "Multiple dipole modeling and localization from spatio-temporal MEG data," *IEEE Transactions on Biomedical Engineering*, vol. 39, no. 6, pp. 541–557, 1992.
- [5] G. Dassios and F. Kariotou, "Magnetoencephalography in ellipsoidal geometry," *Journal of Mathematical Physics*, vol. 44, no. 1, pp. 220–241, 2003.
- [6] F. Kariotou, "Electroencephalography in ellipsoidal geometry," *Journal of Mathematical Analysis and Applications*, vol. 290, no. 1, pp. 324–342, 2004.
- [7] S. N. Giapalaki and F. Kariotou, "The complete ellipsoidal shell-model in EEG imaging," *Abstract and Applied Analysis*, vol. 2006, Article ID 57429, 18 pages, 2006.
- [8] L. D. Landau and E. M. Lifshitz, *Electrodynamics of Continuous Media*. Pergamon, London, 1960.
- [9] J. Malmivuo and R. Plonsey, *Bioelectromagnetism*. Oxford University Press, New York, 1995.
- [10] M. Hämäläinen, R. Hari, R. J. Ilmoniemi, J. Knuutila, and O. . V. Lounasmaa, "Magnetoencephalography— theory, instrumentation, and applications to noninvasive studies of the working human brain," *Reviews of Modern Physics*, vol. 65, no. 2, pp. 413–497, 1993.
- [11] A. Barnard, I. Duck, and M. Lynn, "The application of electromagnetic theory to electrocardiology. I. derivation of the integral equations," *Biophysical Journal*, vol. 7, no. 5, pp. 443–462, 1967.
- [12] E. W. Hobson, *The theory of spherical and ellipsoidal harmonics*. Chelsea, New York, 1955.
- [13] D. Gutiérrez, A. Nehorai, and H. Preissl, "Ellipsoid head model for fetal magnetoencephalography: Forward and inverse solutions," *Physics in Medicine and Biology*, vol. 50, no. 9, pp. 2141–2157, 2005.